PERGAMON

International Journal of Solids and Structures 39 (2002) 5851–5863

INTERNATIONAL JOURNAL OF SOLIDS and STRUCTURES

www.elsevier.com/locate/ijsolstr

Energy approach to a linearization contact problem of simply supported cross-ply laminated composite plate

WeiPing Hu, Xing Zhang *, QingChun Meng

Department of Flight Vehicle Design, Beijing University of Aeronautics and Astronautics, Division 508, Beijing 100083, China

Received 12 January 2001; received in revised form 18 April 2002

Abstract

The nonlinear contact problem of laminated composite plate is linearized by inverse method, i.e. the contact zone and the loading distribution with adjustable parameter on contact zone are assumed to be given to solve the curvature of indenter—a rigid sphere. By means of the principle of superposition, the loading state is decomposed into symmetric state and antisymmetric state. The antisymmetric state is decomposed further to obtain simpler loading state for analysis. The Fourier series and Legendre series are applied to describing the displacement field of contact loading states, and the principle of minimum potential energy is used to determine the unknown coefficients of the above series. Then the displacement and stress fields of the laminated composite plate are known. The adjustable parameter of loading distribution is used to satisfy the compatibility conditions of displacements along the contact surface. By the way the indenter curvature is determined. Then, a series of curves can be figured out after the operation with definite steps. Be based on these curves, the contact zones can be determined from known indenter curvature and the loading. In addition, the glue layers are considered completely the same as other composite plies in this analysis. From the computational results, it can be shown that the displacements and stresses converge very well, and the distributions of shearing and normal stresses obtained from constitutive equation and from equilibrium equation agree with each other very well.

Keywords: Contact problem; Laminated composite plate; Inverse method; Energy-method; Fourier series; Legendre series

1. Introduction

Contact analysis is a difficult task in solid mechanics for its nonlinearity, especially in analysis of composite structures. The classical contact theory—Hertz formula (Hertz, 1881) is based upon assumption of semi-infinite plane or space. Whereas the thickness dimension of each layer in general composite structures are finite comparing with the dimensions of contact zone. Finite element method (Mahajan, 1998; Váradi et al., 1999) and boundary element method (Simunovic and Srdan, 1992), which always lead to a large number of degrees of freedom especially in three-dimensional analysis, are used to solve contact problem. Other various methods (see e.g. Ahmadi et al., 1983; Keer and Miller, 1983; Sankar, 1989; Wu and Yen, 1994) are applied by using approximate or exact Green's function. These methods are complex for

* Corresponding author. Fax: +86-10-82315644.
E-mail address: xingzhangbuaa@sina.com (X. Zhang).

0020-7683/02/$ - see front matter
PII: S0020-7683(02)00376-1

solving the nonlinear problem straightly, moreover, the thickness and rigidity of glue layers are assumed to be zero and infinite respectively. However, in analysis of damage mechanics of composite structures, it is very important to know the damage coupled distribution of stresses of glue layers, because many composite structures are failed from the delamination cracks created by shearing stress or normal stress on the interface between glue layer and composite ply. Interface constitutive laws have been mainly used in the study of contact problems, fracture mechanics for concrete, adhesive films, homogeneized behavior of composite and of composite delamination. The use of interface models in the analysis of composite delamination has been proposed by Allix (1989), and developed in Allix et al. (1991), Ladevèze (1992), Allix and Ladevèze (1992). In these works the schematization of the laminated proposed by Ladevèze is used. In this paper the thickness and rigidity of glue layers are considered completely the same as other composite plies. To simplify the analysis, the generalized parabolic pressure distribution with an adjustable parameter is applied to simulating the actual pressure distribution. To avoid the complexity of nonlinear problem, inverse method is applied, namely the loading distribution with adjustable parameter and contact zone are assumed to be known and the curvature of indenter is to be solved. In this paper, to consider the analysis of delamination damage and fatigue life prediction further, energy method is applied instead of exact solution (Pagano, 1970). The results show the displacements and stresses converge very well, further more, the distribution of shearing stresses and normal stress obtained from constitutive equation agree with that obtained from equilibrium equation very well.

2. The decomposition of loading state

Figs. 1 and 2 show a symmetrically laminated composite plate of simple supports pressed by a rigid sphere at the mid-point of upper surface. The curvature of rigid sphere is κ.

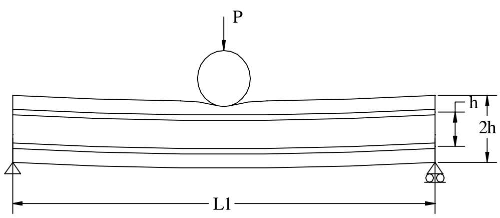

Fig. 1. The original loading state of laminated composite plate.

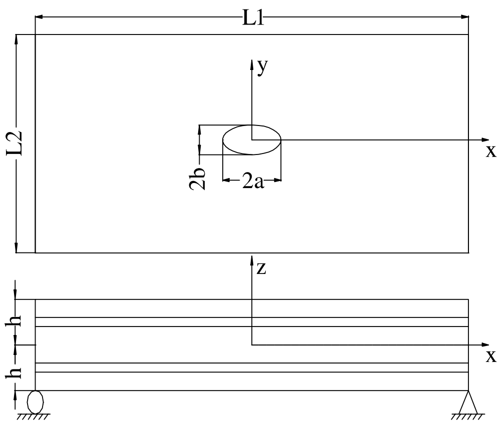

Fig. 2. A laminated composite plate with an indention of elliptic projection.

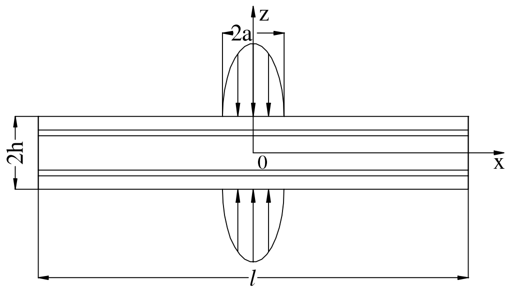

Fig. 3. The symmetric loading state $\langle\alpha\rangle$.

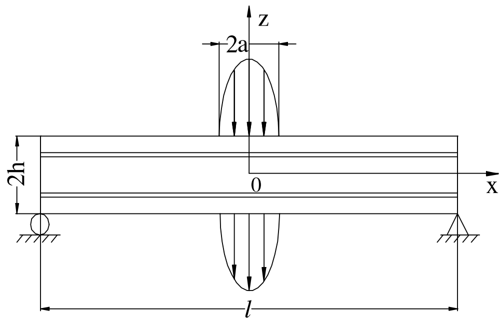

Fig. 4. The antisymmetric loading state $\langle\beta\rangle$.

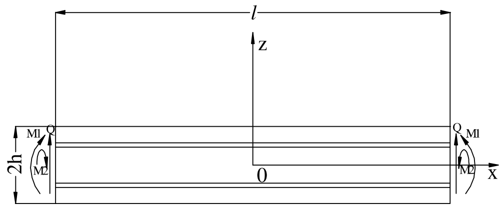

Fig. 5. The additional loading state $\langle\gamma\rangle$.

The loading state is decomposed into symmetric state and antisymmetric state. According to the principle of Sanit–Venant, the symmetric state can be simplified as the symmetric state $\langle\alpha\rangle$ further, which is shown in Fig. 3. Similarly, the antisymmetric state can be decomposed into the antisymmetric loading state $\langle\beta\rangle$ and the additional loading state $\langle\gamma\rangle$ further, which are shown in Figs. 4 and 5 respectively.

3. The analysis of the symmetric loading state

3.1. The further simplification for the mechanics model of symmetric loading state

The dimensions of contact zone and the plate thickness are very small in comparison with the width and length of laminated plate. Then the stress field of plate under the above symmetric loading has obvious local effects. According to Saint–Venant's principle, the analysis is only needed in the internal part of plate and the external part can be considered as stress free. The loading state of internal square part with span l determined from Saint–Venant's principle is shown in Fig. 3.

3.2. Displacements field

The laminated plate is subjected to transverse load that is symmetrical about x-axis, y-axis and z-axis. So, w is the even function of x and y, while the odd function of z, and u is the odd function of x, while the even function of y and z, and v is the odd function of y, while the even function of x and z. Then the displacement field can be described as follows

$$\left.\begin{aligned} w^{(k)}(x,y,z) &= \textstyle\sum_{m,n,p} C^{(k)}_{mnp} f_m(x) f_n(y) g_p(z) \\ u^{(k)}(x,y,z) &= \textstyle\sum_{m,n,p} A^{(k)}_{mnp} s_m(x) f_n(y) t_p(z) \\ v^{(k)}(x,y,z) &= \textstyle\sum_{m,n,p} B^{(k)}_{mnp} f_m(x) s_n(y) t_p(z) \end{aligned}\right\} \tag{1}$$

where $m, n, p = 1, 2, 3, \ldots,$ is the code of each function term in series; k is the sequence number of every composite ply or glue layer and it has the same meaning in following equations; $A^{(k)}_{mnp}$, $B^{(k)}_{mnp}$ and $C^{(k)}_{mnp}$ are the unknown generalized displacements; and

$$f_m(x) = (-1)^{m+1} \cos\left(\frac{2m-1}{l}\pi x\right) \quad s_m(x) = (-1)^m \sin\left(\frac{2m-1}{l}\pi x\right)$$

$$f_n(y) = (-1)^{n+1} \cos\left(\frac{2n-1}{l}\pi y\right) \quad s_n(y) = (-1)^n \sin\left(\frac{2n-1}{l}\pi y\right)$$

$$g_p(z) = P_{2p-1}\left(\frac{z}{h}\right) = \sum_{i=0}^{p-1} \frac{(-1)^i (4p-2i-2)!}{2^{2p-1} i!(2p-i-1)!(2p-2i-1)!} \left(\frac{z}{h}\right)^{2p-2i-1}$$

$$t_p(z) = P_{2p-2}\left(\frac{z}{h}\right) = \sum_{i=0}^{p-1} \frac{(-1)^i (4p-2i-4)!}{2^{2p-2} i!(2p-i-2)!(2p-2i-2)!} \left(\frac{z}{h}\right)^{2p-2i-2}$$

where, $P(z/h)$ is the Legendre function.

3.3. The distribution of contact pressure

The distribution of contact pressure on the upper surface can be expressed by following function:

$$p(x,y) = \begin{cases} p_0\left[1 - \left(\frac{x}{a}\right)^{\overline{m}}\right]\left[1 - \frac{(y/b)^{\overline{m}}}{\left(\sqrt{1-(x/a)^2}\right)^{\overline{m}}}\right] & x \in \Omega, \quad \overline{m} \in [2,4,6,\ldots] \\ 0 & x \notin \Omega \end{cases} \tag{2}$$

where p_0 is the maximum pressure intensity, a and b are the semi-major axis and semi-minor axis of contact area respectively, $\overline{m}$ is defined as loading exponent determined by the compatibility conditions of displacements within the contact surface in Section 6. Ω denotes the contact zone. From Eq. (2), the relationship between total load P and maximum pressure intensity p_0 can be expressed by following function:

$$P = 8abp_0 \int_0^1 \int_0^{\sqrt{1-(\bar{x})^2}} \left(1 - (\bar{x})^{\overline{m}}\right) \left[1 - \frac{(\bar{y})^{\overline{m}}}{\left(\sqrt{1-(\bar{x})^2}\right)^{\overline{m}}} \right] \mathrm{d}\bar{x}\,\mathrm{d}\bar{y} \tag{3}$$

where, $\bar{x} = x/a$, $\bar{y} = y/b$.

The contact load can be expanded by Fourier series:

$$p(x,y) = \sum_{m,n} p_{mn}(x,y)(-1)^{m+1} \cos\left(\frac{2m-1}{l}\pi x\right)(-1)^{n+1} \cos\left(\frac{2n-1}{l}\pi y\right) \tag{4}$$

where

$$p_{mn}(x,y) = \frac{4}{l^2} \int_{-a}^{a} \int_{-b\sqrt{1-(x/a)^2}}^{b\sqrt{1-(x/a)^2}} p(x,y)(-1)^{m+1} \cos\left(\frac{2m-1}{l}\pi x\right)(-1)^{n+1} \cos\left(\frac{2n-1}{l}\pi y\right) \mathrm{d}x\,\mathrm{d}y$$

3.4. Energy-method

Now, the generalized displacements $A_{mnp}^{(k)}$, $B_{mnp}^{(k)}$ and $C_{mnp}^{(k)}$ in Eq. (1) will be determined by the principle of minimum potential energy.

The strain energy of laminated plate can be obtained from the following equation

$$U = \sum_k U_k = \sum_k \frac{1}{2} \int_{z_{k-1}}^{z_k} \int_{-l/2}^{l/2} \int_{-l/2}^{l/2} \sigma_{ij}^{(k)} \varepsilon_{ij}^{(k)}\,\mathrm{d}x\,\mathrm{d}y\,\mathrm{d}z \tag{5}$$

The constitutive relations of kth arbitrary composite ply or glue layer can be expressed as:

$$\begin{Bmatrix} \sigma_x^{(k)} \\ \sigma_y^{(k)} \\ \sigma_z^{(k)} \\ \tau_{yz}^{(k)} \\ \tau_{xz}^{(k)} \\ \tau_{xy}^{(k)} \end{Bmatrix} = \begin{bmatrix} Q_{11}^{(k)} & Q_{12}^{(k)} & Q_{13}^{(k)} & Q_{14}^{(k)} & Q_{15}^{(k)} & Q_{16}^{(k)} \\ Q_{12}^{(k)} & Q_{22}^{(k)} & Q_{23}^{(k)} & Q_{24}^{(k)} & Q_{25}^{(k)} & Q_{26}^{(k)} \\ Q_{13}^{(k)} & Q_{23}^{(k)} & Q_{33}^{(k)} & Q_{34}^{(k)} & Q_{35}^{(k)} & Q_{36}^{(k)} \\ Q_{14}^{(k)} & Q_{24}^{(k)} & Q_{34}^{(k)} & Q_{44}^{(k)} & Q_{45}^{(k)} & Q_{46}^{(k)} \\ Q_{15}^{(k)} & Q_{25}^{(k)} & Q_{35}^{(k)} & Q_{45}^{(k)} & Q_{55}^{(k)} & Q_{56}^{(k)} \\ Q_{16}^{(k)} & Q_{26}^{(k)} & Q_{36}^{(k)} & Q_{46}^{(k)} & Q_{56}^{(k)} & Q_{66}^{(k)} \end{bmatrix} \begin{Bmatrix} \varepsilon_x^{(k)} \\ \varepsilon_y^{(k)} \\ \varepsilon_z^{(k)} \\ \gamma_{yz}^{(k)} \\ \gamma_{xz}^{(k)} \\ \gamma_{xy}^{(k)} \end{Bmatrix} \tag{6}$$

The geometry equation of kth ply or layer is

$$\varepsilon_{ij}^{(k)} = \frac{1}{2}\left(\frac{\partial u_i^{(k)}}{\partial x_j} + \frac{\partial u_j^{(k)}}{\partial x_i}\right) \tag{7}$$

From Eqs. (1) and (5)–(7), the strain energy of kth ply or layer in composite laminate can be expressed as

$$\begin{aligned} U^{(k)} = \frac{1}{2}\Bigg\{ & \sum_{m,n,p,i,j,q} S_{kmnpijq}^{(AA)} A_{mnp}^{(k)} A_{ijq}^{(k)} + \sum_{m,n,p,i,j,q} S_{kmnpijq}^{(AB)} A_{mnp}^{(k)} B_{ijq}^{(k)} + \sum_{m,n,p,i,j,q} S_{kmnpijq}^{(AC)} A_{mnp}^{(k)} C_{ijq}^{(k)} \\ & + \sum_{m,n,p,i,j,q} S_{kmnpijq}^{(BA)} B_{mnp}^{(k)} A_{ijq}^{(k)} + \sum_{m,n,p,i,j,q} S_{kmnpijq}^{(BB)} B_{mnp}^{(k)} B_{ijq}^{(k)} + \sum_{m,n,p,i,j,q} S_{kmnpijq}^{(BC)} B_{mnp}^{(k)} C_{ijq}^{(k)} \\ & + \sum_{m,n,p,i,j,q} S_{kmnpijq}^{(CA)} C_{mn}^{(k)} A_{pq}^{(k)} + \sum_{m,n,p,i,j,q} S_{kmnpijq}^{(CB)} C_{mnp}^{(k)} B_{ijq}^{(k)} + \sum_{m,n,p,i,j,q} S_{kmnpijq}^{(CC)} C_{mnp}^{(k)} C_{ijq}^{(k)} \Bigg\} \end{aligned} \tag{8}$$

where $S_{kmnpijq}^{(AA)}, S_{kmnpijq}^{(AB)}, S_{kmnpijq}^{(AC)}, \ldots, S_{kmnpijq}^{(CC)}$ are known coefficients determined from Eqs. (1), (5)–(7).

The potential energy of external force can be expressed as

$$\begin{aligned} V = &-2\int_{-a}^{a}\int_{-b\sqrt{1-(x/a)^2}}^{b\sqrt{1-(x/a)^2}} p(x,y)\cdot w^{(k_{\max})}(x,y,h)\,\mathrm{d}x\,\mathrm{d}y - 2\int_{-l/2}^{l/2}\int_{-h}^{h}\sigma_x\left(\frac{l}{2},y,z\right)\cdot u\left(\frac{l}{2},y,z\right)\mathrm{d}z\,\mathrm{d}y \\ &-2\int_{-l/2}^{l/2}\int_{-h}^{h}\tau_{xy}\left(\frac{l}{2},y,z\right)\cdot v\left(\frac{l}{2},y,z\right)\mathrm{d}z\,\mathrm{d}y - 2\int_{-l/2}^{l/2}\int_{-h}^{h}\tau_{xz}\left(\frac{l}{2},y,z\right)\cdot w\left(\frac{l}{2},y,z\right)\mathrm{d}z\,\mathrm{d}y \\ &-2\int_{-l/2}^{l/2}\int_{-h}^{h}\tau_{yx}\left(x,\frac{l}{2},z\right)\cdot u\left(x,\frac{l}{2},z\right)\mathrm{d}z\,\mathrm{d}x - 2\int_{-l/2}^{l/2}\int_{-h}^{h}\sigma_y\left(x,\frac{l}{2},z\right)\cdot v\left(x,\frac{l}{2},z\right)\mathrm{d}z\,\mathrm{d}x \\ &-2\int_{-l/2}^{l/2}\int_{-h}^{h}\tau_{yz}\left(x,\frac{l}{2},z\right)\cdot w\left(x,\frac{l}{2},z\right)\mathrm{d}z\,\mathrm{d}x \end{aligned} \tag{9}$$

where $k_{\max}$ is the sequence number of the outmost composite ply.

On the interface between the kth layer and the $k+1$th layer, the conditions of continuity must be satisfied by the displacement and surface force. So an additional term should be included in the functional of total potential energy as

$$J^{(k,k+1)} = \int_{S^*}\left[\left(u^{(k+1)}-u^{(k)}\right)\tau_{xz}^{(k)} + \left(v^{(k+1)}-v^{(k)}\right)\tau_{yz}^{(k)} + \left(w^{(k+1)}-w^{(k)}\right)\sigma_z^{(k)}\right]\mathrm{d}S^* \tag{10}$$

Be based on the principle of multi-zone generalized potential energy, we have

$$\delta\Pi = \delta\left\{\left(\sum_{k=1}^{k_{\max}}U^{(k)} + \sum_{k=1}^{k_{\max}-1}J^{(k,k+1)}\right) + V\right\} = 0 \tag{11}$$

According to Eq. (11), a system of equations about generalized displacements $A_{mnp}^{(k)}$, $B_{mnp}^{(k)}$ and $C_{mnp}^{(k)}$ can be obtained as follows

$$\left.\begin{aligned} \sum\nolimits_{k,i,j,q}T_{kmnpijq}^{(AA)}\cdot A_{ijq}^{(k)} + \sum\nolimits_{k,i,j,q}T_{kmnpijq}^{(AB)}\cdot B_{ijq}^{(k)} + \sum\nolimits_{k,i,j,q}T_{kmnpijq}^{(AC)}\cdot C_{ijq}^{(k)} = 0 \\ \sum\nolimits_{k,i,j,q}T_{kmnpijq}^{(BA)}\cdot A_{ijq}^{(k)} + \sum\nolimits_{k,i,j,q}T_{kmnpijq}^{(BB)}\cdot B_{ijq}^{(k)} + \sum\nolimits_{k,i,j,q}T_{kmnpijq}^{(BC)}\cdot C_{ijq}^{(k)} = 0 \\ \sum\nolimits_{k,i,j,q}T_{kmnpijq}^{(CA)}\cdot A_{ijq}^{(k)} + \sum\nolimits_{k,i,j,q}T_{kmnpijq}^{(CB)}\cdot B_{ijq}^{(k)} + \sum\nolimits_{k,i,j,q}T_{kmnpijq}^{(CC)}\cdot C_{ijq}^{(k)} = R_{kmnp} \end{aligned}\right\} \tag{12}$$

$(k = 1,2,\ldots,k_{\max},\ \ m,i = 1,2,3,\ldots,M,\ \ n,j = 1,2,3,\ldots,N,\ \ p,q = 1,2,3,\ldots,NP)$.

Then $A_{mnp}^{(k)}$, $B_{mnp}^{(k)}$ and $C_{mnp}^{(k)}$ can be determined by solving above system of equations. The displacement components, strain and stress components are determined also. M, N are given by Eq. (4) and NP will be determined by convergence test of stress components.

4. The analysis of the antisymmetric loading state

4.1. The further simplification for the mechanical model of antisymmetric loading state

Then we discuss the stress field of plate under the antisymmetric loading. According to the Saint–Venant's principle, the analysis is only needed in the internal part of plate and the external part can be analyzed in classical laminated composite plate theory. Further more, in the contact effect zone, the antisymmetric loading can be decomposed into the loading state of simply supported plate shown in Fig. 4 and the additional loading state with boundary conditions of static force shown in Fig. 5.

4.2. The solutions for the antisymmetric loading state $\langle\beta\rangle$

In displacement field expressions of this loading state, all the functions except for $t_p(z)$ and $g_p(z)$, which are expressed in Eq. (13), are the same with Eq. (1)

$$\left.\begin{aligned} g_p(z) &= P_{2p-2}\left(\frac{z}{h}\right) = \sum_{i=0}^{p-1} \frac{(-1)^i(4p-2i-4)!}{2^{2p-2}i!(2p-i-2)!(2p-2i-2)!}\left(\frac{z}{h}\right)^{2p-2i-2} \\ t_p(z) &= P_{2p-1}\left(\frac{z}{h}\right) = \sum_{i=0}^{p-1} \frac{(-1)^i(4p-2i-2)!}{2^{2p-1}i!(2p-i-1)!(2p-2i-1)!}\left(\frac{z}{h}\right)^{2p-2i-1} \end{aligned}\right\} \tag{13}$$

To solve the unknown generalized displacements in the displacement field expression of this loading state, it is just needed to take the same steps that have been done in Section 3.

4.3. The solutions for the additional loading state $\langle\gamma\rangle$

In the additional loading state shown in Fig. 5, the plate is subjected to the symmetrical static force on every boundary. The classical laminated plate theory is used and the displacement field can be described as follows

$$\left.\begin{aligned} w &= \sum_{m,n} \overline{C}_{mn}\left[\cos\left(\frac{2m-1}{l}\pi x\right)\cos\left(\frac{2n-1}{l}\pi y\right) + \cos\left(\frac{2m-1}{l}\pi x\right) + \cos\left(\frac{2n-1}{l}\pi y\right)\right] \\ u &= -\frac{\partial w}{\partial x}z = \sum_{m,n} \overline{C}_{mn}\left(\frac{2m-1}{l}\pi\right)\sin\left(\frac{2m-1}{l}\pi x\right)\left[\cos\left(\frac{2n-1}{l}\pi y\right) + 1\right]\cdot z \\ v &= -\frac{\partial w}{\partial y}z = \sum_{m,n} \overline{C}_{mn}\left(\frac{2n-1}{l}\pi\right)\left[\cos\left(\frac{2m-1}{l}\pi x\right) + 1\right]\sin\left(\frac{2n-1}{l}\pi y\right)\cdot z \end{aligned}\right\} \tag{14}$$

where, $m, n = 1, 2, 3, \ldots,$ is the sequence number of each function term in series. $\overline{C}_{mn}$ is the unknown generalized displacement.

The force on the boundaries is the difference between two states. One state is the stress solutions on the boundary sections of Saint–Venant's zone from solving the original plate of simple supports subjected to the concentrated force on it's center point, and the other state is the stress solutions on the boundaries of plate (the span of which is the same with that of Saint–Venant's zone) from solving the loading state which is same as the one shown in Fig. 4 expect that it is subjected to the concentrated load instead of distributive one on it's center point. These two states of stress solutions can be obtained straightly from Levy's solutions. Then the principle of minimum potential energy is used to determine the generalized displacement $\overline{C}_{mn}$ in Eq. (14).

5. Equations of displacement compatibility in the contact zone

Due to the high rigidity of the metallic sphere in comparison with the composite laminated plate, the contact sphere is assumed to be a rigid body. Furthermore, for the simplicity of analysis, the equations of displacement compatibility are established along the major and minor axis of the elliptical contact zone, on the basis of the least-square method. Then the following quantity and equation will be introduced,

$$\begin{aligned} \Delta^2 &= \Delta_1^2 + \Delta_2^2 \\ &= \int_0^a \left\{(w(0,0,h) - w(x,0,h)) - \frac{1}{2}\kappa x^2\right\}^2 \mathrm{d}x + \int_0^b \left\{(w(0,0,h) - w(0,y,h)) - \frac{1}{2}\kappa y^2\right\}^2 \mathrm{d}y \end{aligned} \tag{15}$$

$$\frac{\partial \Delta^2}{\partial \kappa} = \frac{1}{10}(a^5 + b^5)\kappa + \int_0^a w(0,0,h)x^2\,\mathrm{d}x + \int_0^b w(0,0,h)y^2\,\mathrm{d}y - \int_0^a w(x,0,h)x^2\,\mathrm{d}x - \int_0^b w(0,y,h)y^2\,\mathrm{d}y = 0 \tag{16}$$

where $w(0,0,h)$ is the deflection of plate at the mid-point of the contact zone, $w(x,0,h)$ and $w(0,y,h)$ are the deflections of plate at the arbitrary points along x-axis and y-axis respectively in contact zone, κ is the curvature of the rigid sphere. Then $\overline{m}$ in Eq. (2), the corresponding value of κ and the ratio a/b between semi-major axis a and semi-minor axis b are determined by the minimum condition of Eq. (15). This minimum condition can be considered as the equation of displacement compatibility in the contact zone in the sense of least-square method.

6. The solution of inverse method for contact problem

The solution of the contact problem is performed by inverse method, on the basis of the analysis given above, through the following procedure:

(a) give a total load P;
(b) give a sequence of value $\overline{m}$;
(c) for each value of $\overline{m}$ give a series of value b/h;
(d) for each value of b/h give a series of value a/b;
(e) establish the relationship between curvature κ of sphere and a/b by means of the minimum condition of Δ for each $\overline{m}$ and a series of value b/h;
(f) on the basis of above relationship, draw a family of curves of $\Delta - a/b$, for each $\overline{m}$ and a series of value b/h;
(g) determine the sequence of a/b and the corresponding curvature κ obtained by the minimum condition of Δ from the above family of curves for the given values of b/h. That is to say, a set of known P and b/h determine an unique value a/b and the corresponding curvature κ;
(h) draw the curve $P - \kappa$ under different b/h;
(i) based on the fact that P is in direct proportion to the κ under a given contact zone, simplify the above curves into the form of curve about relationship between b/h and P/κ.

So the contact zone can be determined from the above curves in practical application. Further, the displacement and stress fields are determined also. Figs. 12–15 are the typical examples of above curves used to determine the contact zone.

7. Example

To verify the availability of above method, a typical example is presented.

The plate is an orthotropic laminated plate. The constants of each composite ply are given as

$$E_1 = E_0, \quad E_2 = 0.3E_0, \quad E_3 = 0.6E_0, \quad G_{12} = 0.16E_0, \quad G_{13} = 0.3E_0, \quad G_{23} = 0.2E_0,$$
$$\mu_{12} = 0.3, \quad \mu_{13} = 0.3, \quad \mu_{23} = 0.3.$$

The length, width and height of original plate are $L1 = 50h$, $L2 = 40h$ and $H = 2h$ respectively. The composite laminates are symmetrical about x-axis and y-axis. The sequence of laminate angle is 0°/90°/0°. The thickness of each composite laminate is $0.4875h/0.975h/0.4875h$. The thickness of each glue layer is $0.025h$.

The glue layer is isotropic and the material constants are given as

$$E_g = 0.021E_0, \quad \mu_g = 0.30.$$

Table 1
The convergence tests of deflection and stresses of the plate and curvature of the rigid sphere

NP	$w(0,0,h)/h$	$h\kappa$	$\sigma_x(0,0,h)/E_0$	$\sigma_y(0,0,h)/E_0$	$\sigma_z(0,0h)/E_0$	$\tau_{xy}(l/4,l/4,z_1)/E_0$
1	−5.64419E−03	2.79185E−02	−8.72581E−04	−5.47431E−04	0.00000E + 00	−2.36667E−06
2	−6.80141E−03	4.78470E−02	−4.87995E−03	−2.97110E−03	−1.37227E−03	3.17970E−05
3	−7.08910E−03	5.16275E−02	−6.24200E−03	−3.65161E−03	−5.78324E−03	2.66613E−05
4	−7.23713E−03	5.38969E−02	−6.52268E−03	−3.58604E−03	−6.64762E−03	2.65833E−05
5	−7.24583E−03	5.37297E−02	−6.10267E−03	−3.30684E−03	−6.05526E−03	2.65859E−05
6	−7.24509E−03	5.35982E−02	−6.11963E−03	−3.39118E−03	−5.35307E−03	2.65868E−05
7	−7.24530E−03	5.35914E−02	−6.08061E−03	−3.37749E−03	−5.58899E−03	2.65871E−05
8	−7.24542E−03	5.35945E−02	−6.10598E−03	−3.40124E−03	−5.52380E−03	2.65871E−05
9	−7.24544E−03	5.35951E−02	−6.09652E−03	−3.39349E−03	−5.58922E−03	2.65871E−05
10	−7.24545E−03	5.35951E−02	−6.10018E−03	−3.39657E−03	−5.56567E−03	2.65870E−05

Note: $z_1 = 0.4875h$.

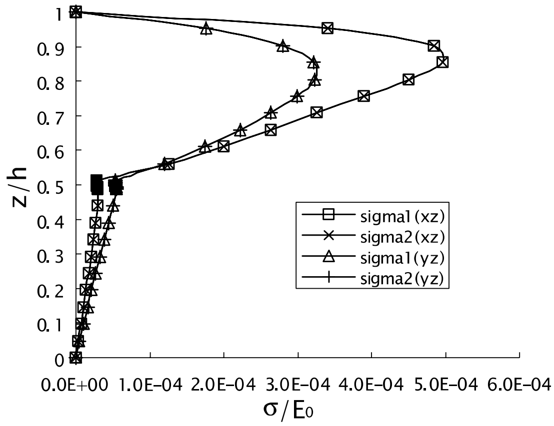

Fig. 6. The distribution of shearing stresses on the section of $(l/40, l/40, z)$ in symmetric loading state.

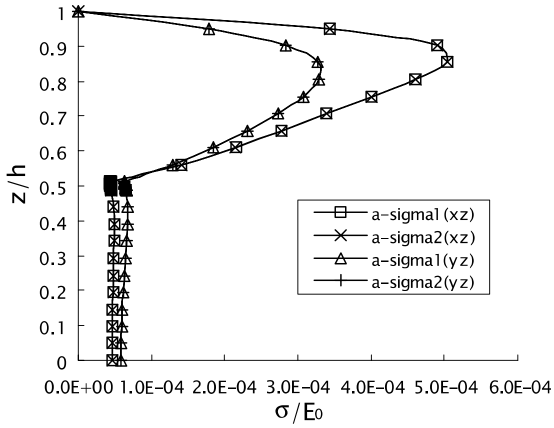

Fig. 7. The distribution of shearing stresses on the section of $(l/40, l/40, z)$ in antisymmetric loading state.

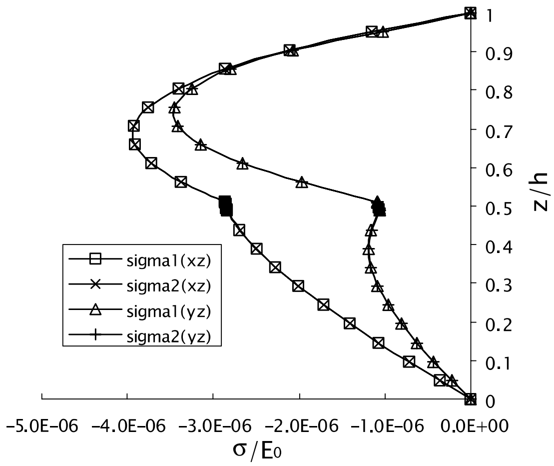

Fig. 8. The distribution of shearing stresses on the section of $(l/4, l/4, z)$ in symmetric loading state.

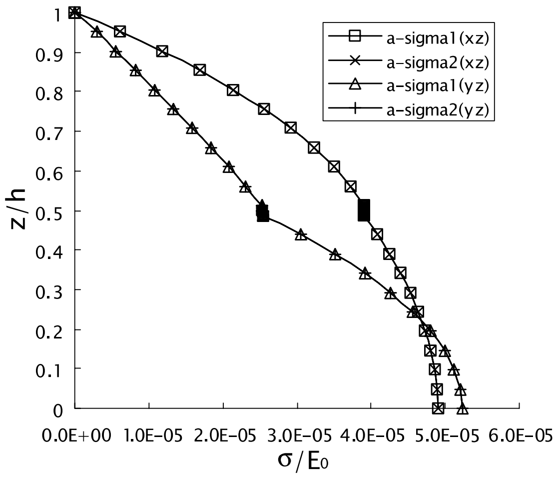

Fig. 9. The distribution of shearing stresses on the section of $(l/4, l/4, z)$ in antisymmetric loading state.

The total external loading is $P = 1.0e - 3E_0h^2$. The parameters of contact zone are given as $b = 0.3h$ and $a/b = 0.9$. The span of square Saint–Venant's effective zone $l = 16b$.

The convergence tests of deflection, stress of plate and the curvature of sphere are shown in Table 1.

The distributions of stresses can be obtained also. They are shown in Figs. 6–11. [1] In these figures, the distributions of shearing and normal stresses obtained from constitutive equation and from equilibrium equation nearly coincide with each other.

[1] Note: In Figs. 6 and 8, "sigma1(xz)" and "sigma2(xz)" denote the τ_{xz} obtained from the constitutive equation and from the equilibrium equation respectively in the symmetric loading state. In Figs. 7 and 9, "a-sigma1(xz)" and "a-sigma2(xz)" denote the τ_{xz} obtained from the constitutive equation and from the equilibrium equation respectively in the antisymmetric loading state. The meanings of other denotations can be deduced from above rule.

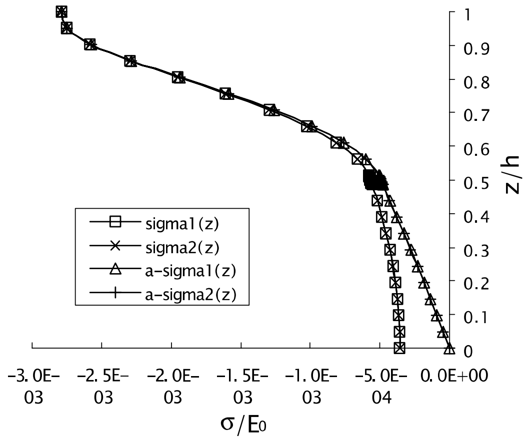

Fig. 10. The distribution of normal stress on the section of $(0, 0, z)$ in symmetric and antisymmetric loading states.

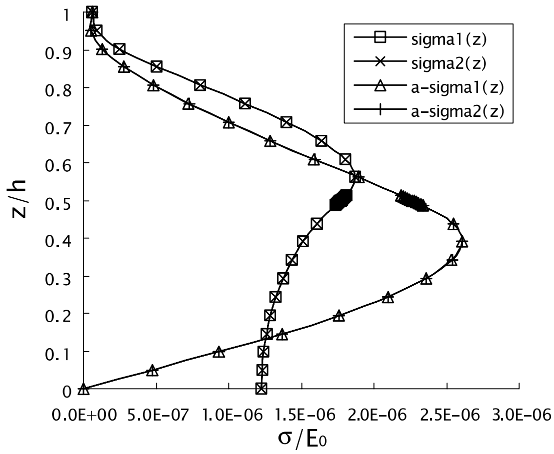

Fig. 11. The distribution of normal stress on the section of $(l/4, l/4, z)$ in symmetric and antisymmetric loading states.

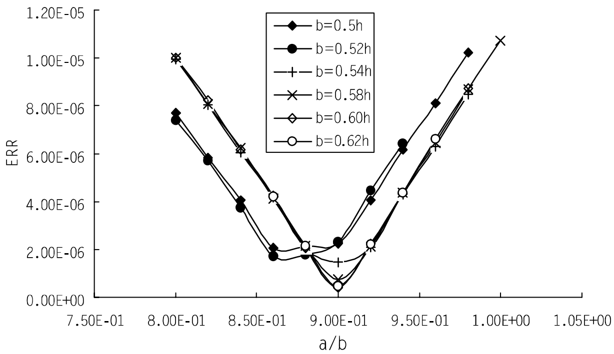

Fig. 12. Δ–a/b curves under different b.

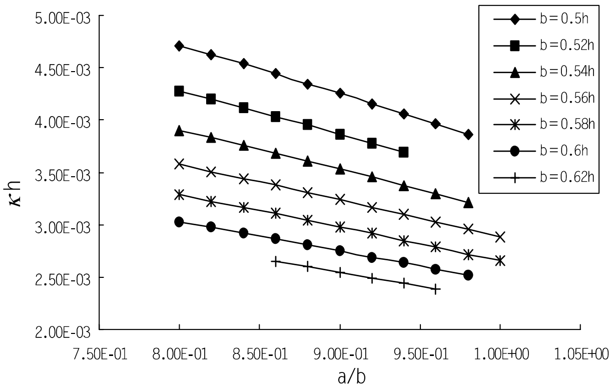

Fig. 13. κ–a/b curves under different b.

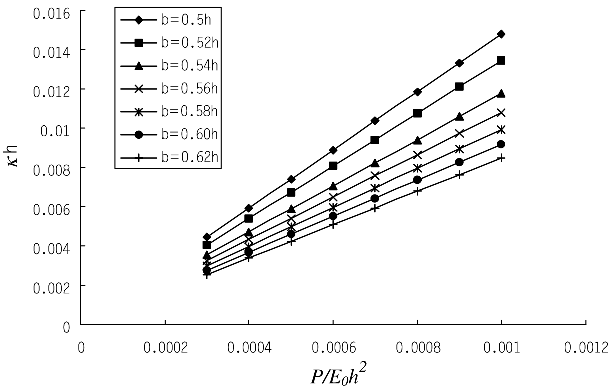

Fig. 14. κ–P curves under different b.

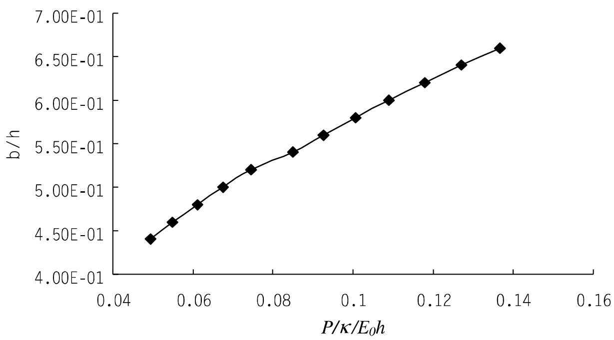

Fig. 15. b–P/κ curve obtained by inverse method.

For the simplicity of the analysis, the value of $\overline{m}$ is assumed to have been determined in the example. The Figs. 12–15 are the curves obtained from the procedure in Section 6. Finally the contact zone can be determined from the Figs 12 and 15 under the given total load P and the curvature κ of rigid sphere.

8. Conclusion

From above analysis, it can be concluded that:

(1) The nonlinear contact problem of laminated composite plate is linearized by inverse method, that is to say, the loading distribution and contact zone are assumed to be given firstly, and the curvature of rigid sphere is to be solved under compatibility conditions of displacements within the contact surface.
(2) The original problem is simplified by means of the principle of superposition and that of Saint–Venant. Each decomposed loading state can be solved in simpler way.
(3) The Fourier series and Legendre series are applied to describe the displacement fields of two loading states needed to be analyzed in contact problem, and the principle of multi-zone generalized potential energy are used to determine the unknown generalized displacements. The additional loading state can be analyzed in terms of classical laminated plate theory. Then the displacement and stress fields of the laminated composite plate are solved.
(4) From the computational results, it can be shown that the distributions of shearing and normal stresses obtained from constitutive equation and from equilibrium equation agree with each other very well.
(5) Through the inverse method, the contact zone can be determined from the known indenter curvature and the total load.
(6) This model can be applied to damage analysis of delaminated failure.

References

Ahmadi, N., Keer, L.M., Mura, T., 1983. Non-Hertzian contact stress analysis for an elastic half space-normal and sliding contact. In: Cairns, D.S. (Ed.), Int. J. Solids 19 (4), 357–373.

Allix, O., 1989. Delaminage par la mécanique de l'endommagement. In: Fouet, J.M., Ladevèze, P., Ohayon, R. (Eds.), Calcule des Structures et Intelligence Artificielle, vol. 1, Pluralis, Paris.

Allix, O., Daudeville, L., Ladevèze, P., 1991. Delamination and damage mechanics. In: Baptiste, D. (Ed.), Mechanics and mechanisms of damage in composites and multi-materials. Mep, London.

Allix, O., Ladevèze, P., 1992. Interlaminar interface modelling for the prediction of delamination. International Journal of Composites and Structures 22 (4), 235–242.

Hertz, H., 1881. Uber die Beruhrung fester Elastischer Korper, Journal for die reine und angewandte mathematik, vol. 92, translated by Jones, D.E., Schott, G.A., MachMillan and Co., London, 1896, pp. 156–171.

Keer, L.M., Miller, G.R., 1983. Smooth indentation of a finite layer. ASCE Journal of Engineering Mechanics 109, 706–717.

Ladevèze, P., 1992. Damage computational method for composite structures. Computers and Structures 44 (1–2), 79–87.

Mahajan, P., 1998. Contact behavior of an orthotropic laminated beam indented by a rigid cylinder. Composite Science and Technology 58, 505–513.

Pagano, N.J., 1970. Exact solutions for rectangular bidirectional composites and sandwich plates. Journal of Composite Materials 4, 20–34.

Sankar, B.V., 1989. Smooth indentation of orthotropic beam. Composites Science and Technology 34, 95–111.

Simunovic, Srdan, 1992. Frictionless contact with BEM using quadratic programming. Journal of Engineering Mechanics 118, 1876–1891.

Váradi, K., Néder, Z., Friedrich, K., Flöck, J., 1999. Finite-element analysis of a polymer composite subjected to ball indentation. Composites Science and Technology 59, 271–281.

Wu, E., Yen, C.-S., 1994. The contact behavior between laminated composite plates and rigid spheres. Journal of Applied Mechanics 61, 60–66.